Protein Tracking and Detection of Protein Motion using Atomic Force Microscopy

Neil H. Thomson,* Monika Fritz,*‡ Manfred Radmacher,* Jason P. Cleveland,* Christoph F. Schmidt,§ and Paul K. Hansma*

*Physics Department, University of California, Santa Barbara, California 93106; ‡Marine Science Institute, University of California, Santa Barbara, California 93106; and §Department of Physics and Biophysics Research Division, University of Michigan, Ann Arbor, Michigan 48109 USA

ABSTRACT Height fluctuations over three different proteins, immunoglobulin G, urease, and microtubules, have been measured using an atomic force microscope (AFM) operating in fluid tapping mode. This was achieved by using a protein-tracking system, where the AFM tip was periodically repositioned above a single protein molecule (or structure) as thermal drifting occurred. Height (z-piezo signal) data were taken in 1- or 2-s time slices with the tip over the molecule and compared to data taken on the support. The measured fluctuations were consistently higher when the tip was positioned over the protein, as opposed to the support the protein was adsorbed on. Similar measurements over patches of an amphiphile, where the noise was identical to that on the support, suggest that the noise increase is due to some intrinsic property of proteins and is not a result of different tip-sample interactions over soft samples. The orientation of the adsorbed proteins in these preliminary studies was not known; thus it was not possible to make correlations between the observed motion and specific protein structure or protein function beyond noting that the observed height fluctuations were greater for an antibody (anti-bovine IgG) and an enzyme (urease) than for microtubules.

INTRODUCTION

Atomic force microscopy (AFM) (Binnig et al., 1986; Rugar and Hansma, 1990) has now been applied to a wide variety of biological systems, from whole cells down to smaller structures, such as chromosomes, membranes, proteins, and nucleic acids (for a recent review see Hansma and Hoh, 1994). Imaging of individual globular proteins physisorbed to surfaces has been one of the most challenging tasks to date. The lateral forces generated in contact mode are sufficiently large to sweep weakly adsorbed molecules, such as proteins, across the support during scanning. However, several groups have imaged inherently stable protein membranes at molecular resolution (see Hansma and Hoh, 1994). Other researchers have been successful in imaging a number of different globular proteins physisorbed to mica (Yang et al., 1994). Despite the high resolution that AFM affords, tip convolution always limits the lateral resolution achieved while scanning single molecules adhered to surfaces, producing images in which the molecules have oversized lateral dimensions. This premise holds whether the microscope is operated in contact or tapping mode, in air or in fluid. However, recent work using a cryo-AFM operating at temperatures below 100 K has yielded images of immunoglobulins that show reproducible molecular substructure and distinct orientations of the molecules on the supports (Han et al., 1995).

The ability of the AFM to operate in liquid opens up the possibility of studying biological processes as they occur in native, aqueous environments. With the recent development of tapping mode in fluid (Dreier et al., 1994; Hansma et al., 1994; Putman et al., 1994) it has been possible to image proteins physisorbed to supports in a consistent and reproducible manner (Fritz et al., 1995). Although the lateral resolution in AFM is limited by tip size, the vertical resolution (i.e., height) is in the sub-nanometer range, limited only by cantilever and detector sensitivities. The idea behind the experiments presented here was to utilize the height resolution to detect motion of proteins adsorbed to surfaces.

In the last year or two, the AFM has been used not only as an imaging microscope but as a tool to measure biological processes occurring in real time. Examples of this include monitoring the dynamics and enzyme degradation of DNA (Bezanilla et al., 1994) and measurement of the adhesion forces between ligand-receptor pairs (Florin et al., 1994) and the forces between complementary strands of DNA (Lee et al., 1994). Recent work on imaging porin surfaces in contact mode has indicated that it is possible to monitor conformational changes on 2D protein crystals (Karrasch et al., 1994; Schabert et al., 1995). Height fluctuations over a layer of the enzyme lysozyme have also been monitored while the enzyme was metabolizing its substrate, indicating that it is possible to detect enzyme activity with the AFM (Radmacher et al., 1994a).

It is generally accepted that proteins are not static, but are complex dynamical systems that are continuously moving (Frauenfelder et al., 1991). When proteins fold, they collapse into different glassy states, their lowest energy state being highly degenerate (Frauenfelder and Wolynes, 1994). At low temperatures (below 200 K) the molecules are

Received for publication 30 October 1995 and in final form 8 February 1996.

Address reprint requests to Dr. Neil H. Thomson, Physics Department, University of California, Santa Barbara, CA 93106. Tel.: 805-893-3999; Fax: 805-893-8315; E-mail: thomson@physics.ucsb.edu.

0006-3495/96/05/2421/11 $2.00

frozen into these states, but above 200 K they fluctuate wildly between them, driven by thermal energy (Parak and Frauenfelder, 1993). At room temperature a protein will constantly explore these substates of conformational space. Much work on ligand binding of carbon monoxide to myoglobin, studied by flash photolysis, has indicated a strong connection between protein dynamics and function (Steinbach, 1991; Young et al., 1991). Although myoglobin is used frequently as a model system, it is expected that this behavior is general to all proteins. Indeed, x-ray crystallography studies of proteins cannot always determine the complete structure because rapid movements of parts of the molecule cannot be resolved (Petsko and Ringe, 1984). This movement often occurs at or near the active site. Crystallographic studies are also being extended to try and monitor protein dynamics, by using short exposure times (milliseconds or less) in intense synchrotron beams (Johnson, 1992). It was hoped that these AFM studies would probe the different conformational states available to the protein molecules on the supports.

The three proteins investigated here are structurally and functionally very different. Urease is a metalloenzyme, a homotrimer of molecular mass of about 270 kDa. Each of the subunits carries a nickel-binding site consisiting of two nickel ions. These active sites are somewhat hidden inside the subunits and are only accessible through a narrow channel, as has been determined recently (Jabri et al., 1995). Antibodies are medium-sized molecules (150 kDa) that are thought to be very flexible because of a so-called hinge region connecting the two regions with the active sites (Fab) with the rest of the molecule (Fc). Microtubules are large, rodlike polymeric structures. They are hollow cylinders made of protofilaments, in which α- and β-tubulin subunits bind to each other in a head-to-tail configuration. In vitro experiments showed that they are much stiffer than other filamentous proteins like actin or biopolymers like DNA (Venier et al., 1994). As the structures of these proteins are different, so are their functions. Urease occurs in bacteria and plants and hydrolyses a very small molecule (urea) to produce accessible nitrogen. Antibodies present their active site, usually located on the surface of the molecule, to detect and bind their antigen. Microtubules are a structural polymeric assembly of tubulin proteins, which play a large role in cell movement and meiosis and as "railways" in intracellular transportation.

To monitor height fluctuations over globular proteins, a tracking system was devised to position the AFM tip over individual protein molecules. This enabled height data over a molecule to be recorded in 1- or 2-s time slices. After each data acquisition period, the tip was repositioned back to the top of the protein molecule to compensate for any lateral drifting that may have occurred. These measurements stemmed from AFM studies of height fluctuations on top of the enzyme lysozyme (Radmacher et al., 1994a). In the previous work, the height fluctuations were recorded as the tip drifted over a layer of protein. With the development of a tracking system it has been possible to study single molecules. Three different types of protein were studied in an effort to determine whether characteristic motion from different classes of protein could be observed. Noise measurements were taken over immunoglobulin G, the enzyme urease, and microtubules. Because these proteins have very different functions, it was thought that they might exhibit different motions that could be detected with the AFM. In addition, noise over patches of a synthetic amphiphile, dimethyldioctadecyl ammonium bromide (DODAB), was also measured to ascertain whether increased noise could result from the tip interacting with a soft specimen.

MATERIALS AND METHODS

Instrumentation

The AFM was a commercial instrument (Nanoscope III; Digital Instruments, Santa Barbara, CA). It was operated in the relatively new tapping mode in fluid (Hansma et al., 1994). In this mode, the cantilever is oscillated with amplitudes of 5 to 10 nm and with frequencies ranging from a few kilohertz to tens of kilohertz, depending on the resonant frequency of the cantilever. The AFM tip "taps" the sample gently and prevents the large lateral forces that remove molecules from supports in the conventional contact mode. Imaging in these experiments was carried out with oscillation frequencies between 16 and 35 kHz. The piezo-tube had a maximum xy scan range of 12 μm (D-scanner; Digital Instruments). Imaging was performed at a scan rate of two or three lines per second.

The cantilevers used for imaging and noise measurements were all triangular silicon Ultralevers (Park Scientific Instruments, Sunnyvale, CA). Different-sized cantilevers from two different wafers were used on the different types of sample. The antibodies were imaged with 180-μm-long by 25-μm-wide levers that had a spring constant of 0.10 N/m. The urease molecules were imaged with 180-μm-long by 38-μm-wide levers with spring constants of 0.12 N/m. The microtubules were imaged with two different levers, both 85 μm long, with widths of 28 μm and 18 μm, which had spring constants of 1.4 N/m and 0.90 N/m, respectively. The amphiphile patches were imaged with levers that were 180 μm long by 25 μm wide, but had spring constants of 0.25 N/m. Spring constants were estimated from measuring unloaded resonant frequencies in air using the method of Cleveland et al. (1993). Values of the spring constants for typical resonant frequencies of the different levers quoted from the manufacturer were used to estimate spring constants, using our measured frequencies and assuming a cubed dependence between spring constant and resonant frequency. Variations in the thickness of the levers will affect the spring constant dramatically (this is a cubed dependence). The thickness can vary from wafer to wafer during the manufacture process but remains fairly constant across a single wafer. Therefore, cantilevers with similar lateral dimensions from different wafers can often have significantly different spring constants.

Cantilevers were cleaned before use, to ensure that the tips were not contaminated. The cantilever chips were placed directly underneath a UV pen lamp (Ultraviolet Products, San Gabriel, CA) with a millimeter clearance for at least 30 min. Strong oxidizing agents such as hydrogen peroxide were also used. Cantilever chips were immersed in H_2O_2 for about 5 min and then rinsed with excess propanol and then deionized water (Milli Q; Millipore System, Eugene, OR). This method was very effective but had the disadvantage of removing the reflective gold coating from the silicon cantilevers. Cleaning in H_2O_2 was often carried out before exposing the chips to UV light.

Sample preparation

All of the samples for the microscope were prepared in a similar way. Small volumes (20 μl to 100 μl) of the solutions of protein or DODAB

were deposited on supports and left to incubate for a given time, before rinsing with excess buffer or deionized water. The samples were mounted in the microscope fluid cell while still wet and imaged under buffer or deionized water. The supports were either freshly cleaved mica or silanized glass coverslips.

The glass coverslips (Electron Microscopy Sciences, Fort Washington, PA), 15 mm in diameter, were cleaned thoroughly before silanization. They were ultrasonicated in a saturated solution of KOH in ethanol for 5 min, rinsed with deionized water, and finally ultrasonicated three times in deionized water for 3 min each time. Silanization was carried out with trimethoxysilylpropyl-diethylenetriamine (DETA) (United Chemical Technologies, Bristol, PA). The coverslips were immersed for 2 min in 1% DETA that had been hydrolyzed in 1 mM acetic acid for 5 min. On removal, they were sonicated in excess deionized water for 2 min, and then dried and cured in an oven at 150°C for 15 min.

Lyophilized anti-bovine immunoglobulin G (Sigma, St. Louis, MO) was dissolved in a 5 mM potassium phosphate (KH_2PO_4) buffer at pH 5 with no additional salt, to a concentration of 1 mg/ml. This solution was then diluted down to 1 μg/ml in three steps, each dilution reducing the concentration by a factor of 10. Twenty microliters of the final solution was deposited on freshly cleaved mica and left for 10 to 15 min, and then the support was rinsed with excess KH_2PO_4 buffer.

Urease samples were also prepared from freeze-dried material (Sigma). Lyophilized protein was dissolved in 5 mM KH_2PO_4 buffer at pH 6 with no salt. Again a solution of concentration 1 μg/ml was deposited on freshly cleaved mica. In this case, 100 μl of solution was incubated for 20 min, before the support was rinsed thoroughly with KH_2PO_4 buffer. No additional purification of the protein samples purchased from Sigma was carried out.

Microtubules were prepared from tubulin purified from bovine brain following the method of Williams and Lee (1982). The tubulin was polymerized in PEM 50 buffer (50 mM piperazine-*N,N'*-bis(2-ethanesulfonic acid), 1 mM EGTA, 2 mM $MgCl_2$, 2 mM NaN_3, pH 6.8, with 10 μM Taxol) at a concentration of 1.2 mg/ml at 37°C for 10 min. The tubulin solution was allowed to polymerize for an additional 12 h at room temperature after it was removed from the water bath. The polymer solution was centrifuged for 30 min at 14,000 rpm (5415 C, table-top centrifuge; Eppendorf) to remove unpolymerized tubulin. The supernatant was discarded and replaced by the same volume of pure PEM 50 buffer (pH 6.8) and 3 μM taxol and resuspended. Fifty microliters of this solution was adsorbed on DETA-coated glass coverslips for just 1 or 2 s before rinsing vigorously with excess PEM 50 buffer containing 3 μM taxol. Microtubules are long, stiff structures with persistence lengths on the order of millimeters. Because of this, the end of the pipette tip was cut so that a wide aperture prevented damage to the microtubules during deposition.

The amphiphile vesicles were prepared by dissolving dimethyldioctadecyl ammonium bromide (DODAB) (Eastman Kodak Company, Rochester, NY) in chloroform to a concentration of approximately 1 mg/ml. The chloroform was then evaporated and the DODAB thoroughly dried using a stream of dry nitrogen gas. The DODAB crystallizes on the walls of the glass container and can then be dissolved in water to a similar concentration. On dissolving in water, the DODAB forms spherical vesicles with diameters on the micron scale, producing a cloudy solution. To make vesicles with diameters comparable to the protein dimensions (i.e., 10 nm and up), the vesicle solution was sonicated in a high-energy tip sonicator for 10 min (sonic dismembrator, model 300; Fisher). The vesicle solution turns clear during the sonication, as the larger vesicles break up into smaller ones that have diameters less than the wavelength of visible light. To produce patches of bilayers of the surfactant on mica, the 1 mg/ml solution was diluted down to 1 μg/ml using a three-step dilution. Twenty microliters of this solution was deposited on mica and left to stand for 10 min before the support was rinsed with excess deionized water.

Protein tracking

The protein-tracking device was designed to maintain the AFM tip directly above a protein molecule (or other distinct feature) for an indefinite period of time as drifting in the microscope head due to thermal fluctuations occurred. A schematic representation of the set-up is shown in Fig. 3. It consists of a Macintosh computer (Quadra 840AV) interfaced to the Nanoscope III AFM. In this set-up the Nanoscope is used in the usual manner, with the feedback electronics controlling the tip-sample separation. The Macintosh is used to monitor height signals (from the *z*-piezo) and manipulate the scanning by applying external signals in addition to those generated by the Nanoscope. The AFM has a breakout box between the microscope head and the feedback electronics. Different signals from the microscope can be "broken out" and monitored from this box. For the tracking system the *z*-piezo signal (or height signal) is monitored. It is passed through an attenuator and a low-pass filter before being connected to the 16-bit analog-to-digital converter (ADC) of the Macintosh. The attenuator is necessary to reduce the high voltages that can be present on the piezo tube ($\pm$220 V) to a range that the ADC can handle ($\pm$10 V). The low-pass filter with a cutoff frequency of 5 kHz was used to eradicate unwanted high-frequency signals picked up on the *z* signal.

The positioning of the tip was controlled by applying signals from the Macintosh 12-bit digital-to-analog converter (DAC) to two external inputs on the *x*- and *y*-piezo signals. These incorporate variable gain settings to increase the DAC voltages ($\pm$10 V range) to the $\pm$220 V range necessary to move the piezo-tube significant lateral distances. The Macintosh signals are actually added to the Nanoscope *x*- and *y*-signals using summing amplifiers, so the Macintosh effectively produces offset signals that move the sample a few nanometers.

The data acquisition, monitoring of *z* signals, and output of the *x* and *y* offsets were all managed on the Macintosh using Superscope II software (GWI Instruments, Sommerville, MA). This is a modular package in which macro routines can be written to record data and output signals. This software was run in conjunction with a MacAdios II data acquisition board (GWI Instruments) in the Macintosh. Data were sampled at a rate of 1 kHz.

The protein tracking was initiated in the following way. The Nanoscope III AFM was used to zoom in, until a single molecule of interest was present in the image and well centered in the field of view. The scan size in the AFM was then set to zero, i.e., scanning was halted. In this situation, the tip went to the center of the scan and therefore was positioned over the molecule. At this point the tracking program in Superscope II was started. The Macintosh took over scanning, making a cross with the tip: that is, it scanned two lines, one in the *x*-direction and one in the *y*-direction, both passing through the initial tip position. As it scans the *z* signal is monitored and the tip is moved to the position of the maximum height signal along these traces (by moving the sample). This sequence is repeated two more times. Then the tip is left in place, and 1 or 2 s of height signal data are recorded. Afterward, the cross-wise scanning over the molecule is recommenced and the cycle repeated. In this way, a series of height data with the AFM tip positioned over a molecule can be acquired. Data were usually acquired for a total of 20 or 30 s (i.e., 20 or 30 tracking cycles for 1-s data slices). The length of the height data set is only limited by the severity of the thermal drift, the patience of the operator, or the amount of memory and disk space left on the computer.

RESULTS AND DISCUSSION

To investigate height fluctuations over individual protein molecules it was necessary to devise preparation methods that produced homogeneous samples with molecules evenly spaced across the support. The molecular density had to be sufficiently sparse to enable imaging of isolated molecules on the surface with the tip able to contact the support, but dense enough to image many similar molecules in one scan area. As well as a good molecular distribution, it was important that the proteins were well bound to the surface. Weakly adsorbed molecules were pushed along the support in the slow scan direction, despite the fact that the tapping mode was being used (unpublished data). This may seem

counterintuitive; in contact mode one would expect (and observes) that such molecules are scraped away in the fast scan direction. However, in tapping mode the tip contacts the sample intermittently and it is possible that the first contact is on one side of the protein and imparts motion in the slow scan direction.

The sample preparation is affected by four factors: the affinity of the molecule (or other structure) for the support, the concentration and amount of the deposited solution, and the length of incubation time allowed before the sample is rinsed. The affinity of protein molecules for supports can be varied by adjusting the buffer pH and so altering their overall charge characteristics. Mica is a negatively charged surface that will bind positively charged proteins. To ensure good adhesion it is often necessary to keep the pH of the buffer acidic, ensuring protonation of the amino groups. For the antibodies it was necessary to have the buffer at pH 5; with urease, pH 6 was sufficient. The antibody has an isoelectric point of between 6 and 8 (personal communication with Sigma) and the urease about 5 (Reithel, 1971). At these pHs both proteins were bound strongly enough not to be moved by the tip during scanning. This suggests that the urease may have a stronger dipole moment that enables it to bind to the mica at higher pH. The microtubules had to be adsorbed to a positively charged support, DETA-silanized glass, because they are negatively charged protein assemblies at pH 7. Microtubules have been imaged consistently on DETA-silanized glass previously and could not be adsorbed to mica (Fritz et al., 1995). The DODAB amphiphiles are positively charged from the dissociation of the ammonium bromide headgroup. Hence, the vesicles adhere strongly to negative mica supports. Once the adhesion properties of the sample have been determined the density of the adsorbates can be altered by adjusting the concentration, amount of solution deposited, and the incubation time. These parameters are noted in Materials and Methods for each of the different systems studied.

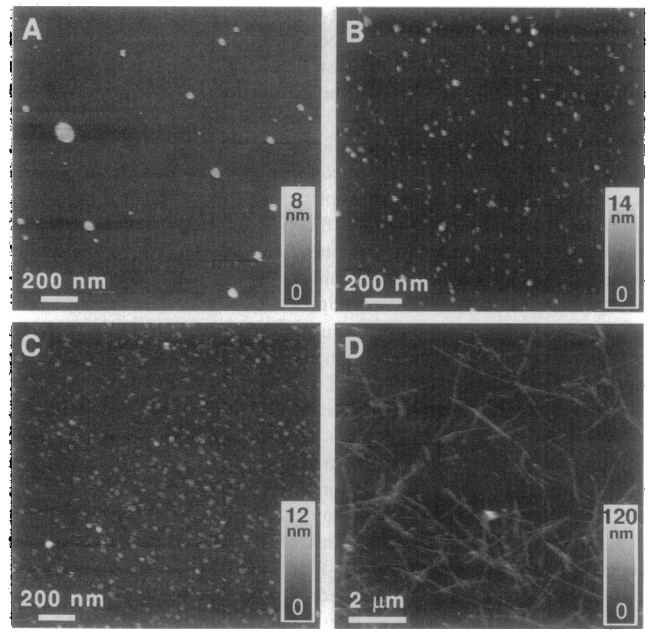

FIGURE 1 AFM images of the different systems used for the motion studies, taken using tapping mode in fluid. (*A*) DODAB amphiphile patches adsorbed to mica and imaged under deionized water. The patches varied in diameter from 10 to 100 or 200 nm. The height of 5 nm indicated that they are bilayer patches and not intact vesicles. (*B*) Anti-bovine IgG molecules on mica imaged under 5 mM KH_2PO_4 buffer at pH 5. Lateral dimensions of the molecules were between 25 and 70 nm, and heights were statistically centred at 3, 3.8, 5, and 7 nm. (*C*) Urease molecules adsorbed to mica and imaged under 5 mM KH_2PO_4 buffer at pH 6. These varied in lateral dimensions from about 40 to 60 nm. Their heights were either 4, 7 to 8, or 15 nm. (*D*) Microtubules adsorbed onto DETA silanized glass imaged under PEM 50 buffer at pH 6.8. The heights of these structures were about 20 to 24 nm, consistent with the expected diameter. Generally, AFM produces images where adsorbates have oversized lateral dimensions due to tip broadening. The heights of biomolecules measured by AFM vary, depending on the operating mode.

Fig. 1 shows typical AFM images obtained on each of the samples used in these studies. Imaging of many similarly sized features in one scan area was used to assay the purity of the globular protein samples. Only particles of certain dimensions were tracked, those that had many other "sisters" of similar dimensions. The DODAB patches varied in size from 10 nm up to 100 or 200 nm in diameter. They had heights of 5 nm, which was consistent with twice the chain length of the DODAB molecules (Okuyama et al., 1988), indicating that the vesicles break on adsorption to the mica to form a bilayer. This could be due to strong interaction between the oppositely charged vesicles and the support. DODAB was chosen as a soft sample because the patches had dimensions comparable to those of the globular proteins. The antibodies showed a distribution of sizes that seemed consistent with Fab and Fc fragments and whole molecules (see Fig. 1 *B*). The lateral dimension of the smallest features was about 25 nm, and that of the largest about 70 nm. Because an antibody molecule is at the very most only 10 nm across, these sizes are due to tip convolution. Using the model of Bustamante et al. (1992) with a parabolic tip of radius 10 nm, a molecule with a 5-nm radius appears to be 30 nm across. The heights of the molecules ranged from 3 to 8 nm, but in histograms of the heights there were definite peaks at 3, 3.8, 5, and 7 nm (unpublished data). It is thought that the smaller values correspond to fragments of molecules and the highest are intact IgG molecules. The highest molecules were always chosen for tracking and noise measurements, because we might expect large conformational changes between different orientations of the Fab domains, relative to the Fc domain. The urease molecules also showed a variation in widths from 40 to 60 nm across. The heights of 90% of the molecules were 4 nm and the others were 7 to 8 nm or 15 nm. Recently the crystal structure of a urease has been determined (Jabri et al., 1995). The molecule is a trimer with T-shaped subunits that are 8 by 8 by 7.5 nm. The whole molecule (trimer) has a diameter of 11 nm. For this reason the molecules that were tracked were those 7 to 8 nm high, in the expectation that these are intact trimers. In actuality this may not be impor-

tant for the observation of motion relating to biological function with urease, because each subunit contains two active nickel centers that metabolize urea. In Fig. 1 *D* the individual microtubules are clearly distinguishable, but little or no detail of their internal strucutre was resolved. This is consistent with previous AFM studies using tapping mode in fluid (Fritz et al., 1995), where the protofilaments were only resolved on a few occasions with exceptional tips. The microtubules often appeared bent, despite their supposed rigid state in natural systems. This is thought to be due to the influence of the taxol during polymerization (Dye et al., 1993).

The dynamics of these systems could be studied using only the AFM, without the tracking set-up. This was achieved by zooming into an area with a single protein, DODAB patch, or microtubule and disabling the slow scan axis (*y*-direction) while scanning the structure. This produces an image in which all of the traces in the *x*-direction are over the same part of the molecule. This type of image is reproduced in Fig. 2 as a three-dimensional projection of the line traces. In the *x*-direction is the length associated with one trace, and the *y*-direction is a measure of the time it takes to acquire 128 line traces. Usually imaging was performed by acquiring data with 512 data points per line and 512 lines. To improve on the temporal resolution in these images, the pixel size was reduced to 128 by 128, at the sacrifice of spatial resolution. The scan speed of an AFM is limited by the reaction time of the piezo-tube and the cantilever response (Butt et al., 1993). The damping of a liquid environment reduces the cantilever response time and increases its effective mass. These images were obtained at the fastest practical scanning speed possible. At higher speeds oscillations could occur and the samples may not have been tracked correctly. It is clear from these plots that the noise on top of the single protein molecules is greater than that over the DODAB patch and the microtubule. In making the comparison between systems, it is important to observe the difference between noise on top of the structures compared with the noise on their supports. The support is defining a standard of noise for any given tip imaging under a certain buffer. If we ask how large the noise is on the proteins compared to the support, we can see that these images suggest that the antibody is the noisiest. The top of the microtubule is not much noisier than the DETA surface, and the noise on the DODAB patch is almost identical to that on the mica. The urease is noisier than the DODAB or microtubule, but probably not as noisy as the antibody. It is difficult to directly compare different systems in these displays because of the different length scales associated with each sample. However, root mean square (RMS) values for the noise on each structure and the support can be obtained from the Nanoscope software. A line can be taken along the *y*-direction of each image both on and off the structures, and the software calculates RMS roughness values. Table 1 shows the range of RMS values obtained on each image in Fig. 2 from the Nanoscope software.

The fact that the noise levels on the mica and the DODAB patch are identical suggests that the increase in the noise over the proteins is due to the inherent properties of the proteins and is not just a result of a different tip-sample interaction over a soft sample. However, this method of acquiring molecular dynamics does not have a very high temporal resolution and is prone to the tip drifting laterally. These *y*-disable plots are useful for visualizing noise differences between molecules and the support, but the time between points on sequential line scans is about 200 ms at best (in the case of the DODAB).

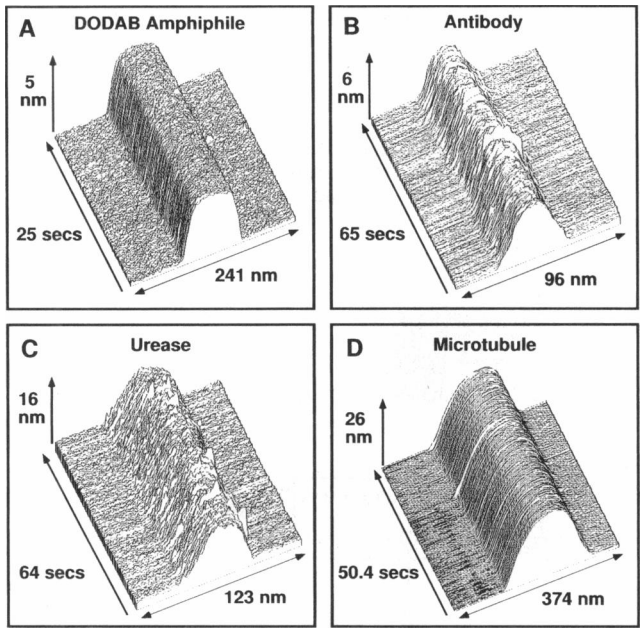

FIGURE 2 Three-dimensional line plots of slow scan axis (*y* direction) disabled AFM images over a single DODAB bilayer patch (*A*), individual protein molecules (*B*, IgG; *C*, urease) and a single microtubule (*D*). Disabling the slow scan direction gives an image that consists of multiple line scans over the same part of the molecule or structure. Therefore, these are time sequences of the topography of one line section through the structure. From this type of image it is possible to monitor the dynamics of molecules, albeit with a low temporal resolution (for example, 200 ms for the DODAB amphiphile). Comparison of noise levels between the support and the top of each structure indicates more height fluctuations over the antibody and urease molecules as compared to the amphiphile patch and the microtubule.

TABLE 1 RMS noise values determined from Nanoscope software for the slow scan disabled images in Fig. 2

	Noise on the support (nm)	Noise on top of the structure (nm)
DODAB/mica	0.07–0.10	0.07–0.10
Antibody/mica	0.15–0.19	0.34–0.43
Urease/mica	0.25–0.33	0.50–0.75
Microtubule/DETA	0.08–0.11	0.21–0.26

Comparison is of noise on top of the DODAB patches and different proteins relative to their supports.

This led to ideas of trying to overcome thermal drift by actively trying to keep the tip over a protein molecule. By using only part of a scan, such as a cross (see Materials and Methods), we can rapidly assess where the molecule is on the support and position the tip accordingly. The tracking set-up is shown schematically in Fig. 3 and has been described in Materials and Methods. Fig. 4 shows typical data that are obtained from tracking a protein molecule. The AFM is used to zoom in on a single molecule with a field of view of 100 nm, say, in the case of urease (Fig. 4 *A*). This image is taken at 128 by 128 pixels, so the acquisition time of an image is smaller, enabling easy centering of the molecule in the image. Once the molecule is centered, the scan size is set to zero and tracking commences. Fig. 4 *B* shows typical traces from the crosswise scanning, which were created while tracking. Each of these traces is recorded before the height data are acquired. These are important for determining whether the AFM is tracking the molecule properly. Fig. 4 *C* shows a history of the lateral movement of the x- and y-piezos necessary to maintain the tip over a urease molecule as drifting occurs. If the drift is severe the tracking system can lose the molecule. From Fig. 4 *C* it is possible to estimate a drift velocity of 0.3 nm/s in this case. Therefore, we can be sure that the tip remains over the protein molecule for the duration of each data slice recording. During each data acquisition period the tip taps at the same place on the molecule; any lateral motion is a consequence of drift. The stepwise jumps of 10 to 15 nm between data acquisition points indicate that the sample has been moved, so that different parts of the tip and protein are in contact. Although urease is only 11 nm in its widest lateral dimension (Jabri et al., 1995), the molecule appears to be at least 40 nm across in the AFM images. Because the tip has a much greater radius of curvature than the protein molecule, we can be certain that the tip is always in contact with the protein molecule when data are recorded. Fig. 4 *D* shows typical traces of the noise data obtained on mica and over urease. These traces are obtained by flattening each data slice and concatenating them.

The tracking system was used on the different types of samples shown in Fig. 1. Fig. 5 shows typical height fluctuations recorded over the different structures and the corresponding noise on the supports. Although the noise on the support is used as the background noise calibration for each sample, one can see that the support noise from sample to sample is very reproducible. Average RMS values of these support traces range from 0.2 to 0.4 nm. These values were calculated by taking the mean squares of each data slice while the tip was over the protein. These 1- or 2-s data slices were first flattened by fitting a line. This would account for any overall drift in the system, whether it is drift in the z-direction or apparent z drift caused by lateral drift across the protein molecule. These mean square values were averaged over the whole concatenated data set and then square

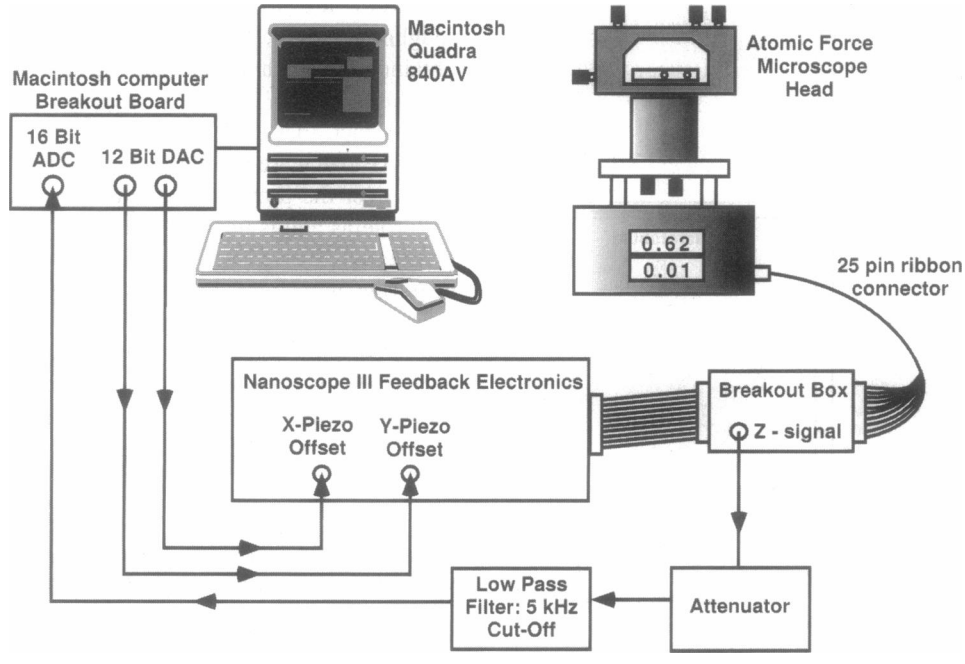

FIGURE 3 Schematic representation of the protein tracking system. This enables the AFM tip to be held for indefinite periods over a single protein molecule while thermal drifting occurs in the microscope head. It consists of a Macintosh computer interfaced to a Digital Instruments Nanoscope III AFM. A molecule of interest is found and positioned in the center of the scan area; then the scan size is set to zero. This moves the tip to the center of the image frame, so that the tip should be positioned over the protein. The Macintosh is then used to scan the piezo-tube in a cross, using offsets applied to the x and y piezo inputs, and monitors the resultant height signal (z signal) over the molecule. The Macintosh then repositions the tip at the place where the height was maximum. This cycle is repeated twice more, and then the tip is left over the molecule, and one or two seconds of the height data over the protein molecule is recorded. Provided that drift is not too severe, the tip can track and record height fluctuations over a single molecule for minutes to hours.

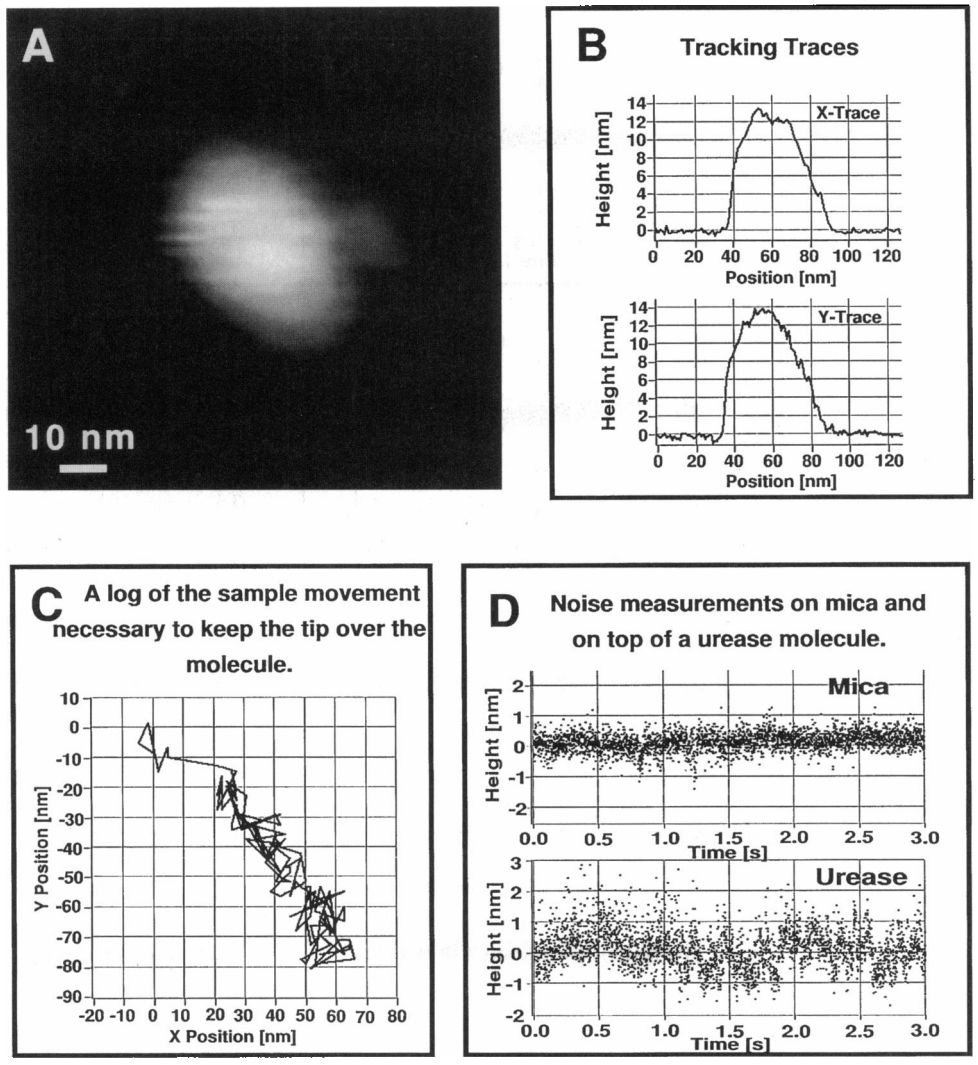

FIGURE 4 An example of data acquired from protein tracking, obtained on a urease sample. (*A*) Typical image of a single protein (urease) molecule before initiating the tracking device. The image is 128 by 128 pixels; lower resolution makes it easier to center the molecule in the field of view. The large lateral dimensions of the molecule are due to tip convolution. (*B*) Line traces recorded over the molecule while the AFM scans the cross. These are the traces just before the 1- or 2-s height fluctuation data slice over the molecule was recorded. (*C*) A plot of the *x* and *y* movement of the piezo-tube required to hold the tip over the molecule during data acquisition. From this history it is possible to estimate lateral drift rates (0.3 nm/s in this case). The 10- to 15-nm jumps indicate that the relative positions of tip and protein are changing from one recording to the next of the 1- or 2-s height fluctuation data slice. However, because the tip has a much larger radius of curvature than the molecule, we can be sure that the tip is still in contact with the protein. This must be true because protein molecules appear broadened in the AFM; for example, urease has an apparent width of at least 40 nm in these studies. (*D*) Typical traces of the height fluctuations recorded on mica and on the urease molecule. The noise on the support is used as a background measurement of noise for a given tip in a given buffer. Comparison of the noise traces shows that there are more fluctuations over the protein. Noise data were taken on the support between protein data sets recorded to ascertain whether the background noise was varying with time. Comparisons of noise data were made between data sets taken immediately after one another, with the same feedback gains and imaging force.

rooted. Table 2 shows RMS values for the data sets shown in Fig. 5.

These were computed for the whole length of the data sets and not just the 3 s shown in Fig. 5. The RMS values also indicate that there is more noise on the proteins than on the support. The RMS value on the DODAB patches is identical to the value on the mica support. Comparing the difference in RMS values for the proteins versus their supports again indicates that there is most movement of the *z*-piezo when the tip is over the antibody and least movement when it is over the microtubule. It is interesting to note that the noise on the DETA-silanized glass is comparable to the mica, even though the DETA may be softer. However, DETA is a short-chain silane and probably packs very densely on the glass surface. Although RMS values give an indication of height fluctuation magnitudes, they do not indicate the frequencies at which most movement is occurring. If we are to relate biological function to measured

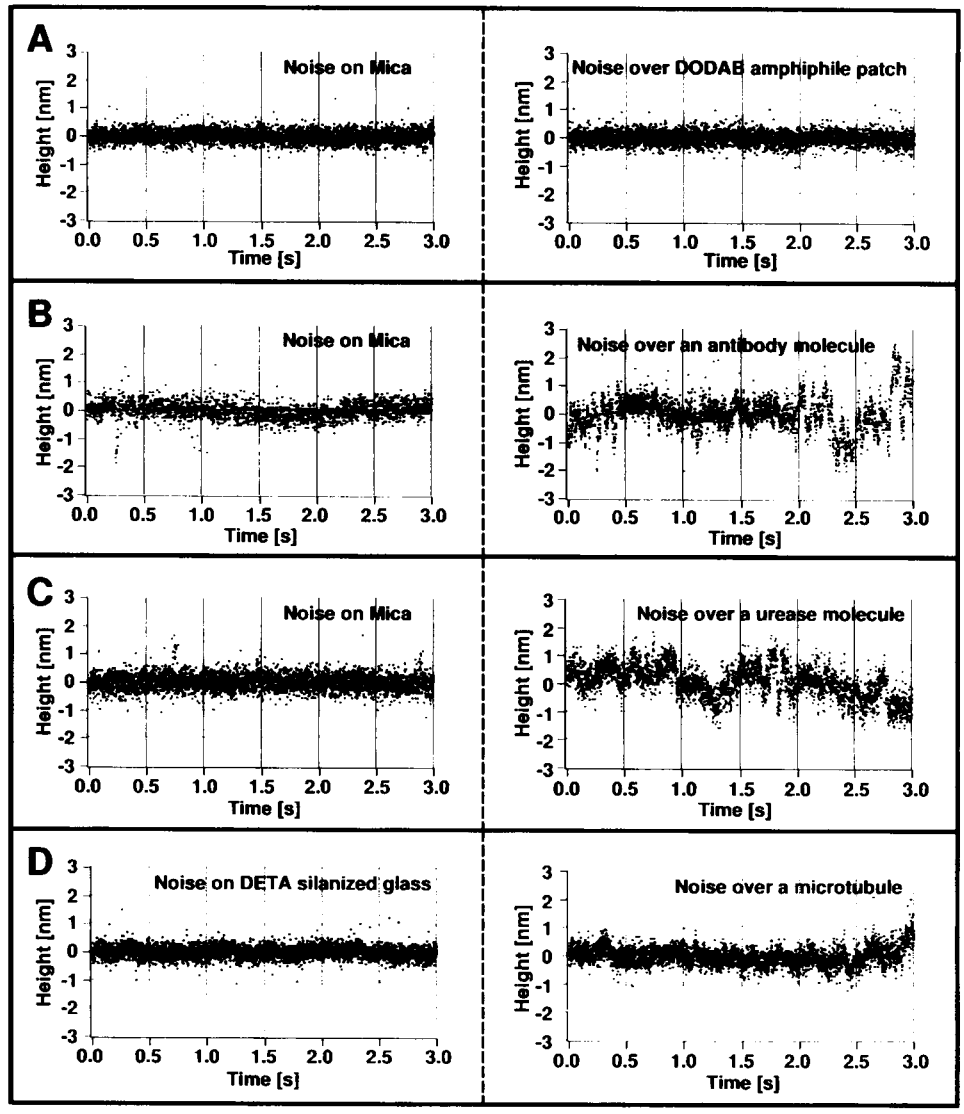

FIGURE 5 Traces of height fluctuations over a DODAB patch (*A*), an antibody molecule (*B*), a urease molecule (*C*), and a microtubule (*D*) as compared with the fluctuations recorded on the supports that the samples were adsorbed on. The noise on the supports was very reproducible, both between different mica samples and from mica to DETA silanized glass. RMS noise values on the supports varied from 0.2 to 0.4 nm. Comparison of these data sets indicates the most fluctuations in height occurring with the tip over the antibody and urease molecules. The traces over the DODAB are indistinguishable from the mica, and the noise over the microtubule appears slightly greater than the DETA support.

TABLE 2 RMS values of the noise data taken with the protein-tracking system shown in Fig. 5

	Noise on the support (nm)	Noise on the structure (nm)
DODAB/mica	0.22	0.22
Antibody/mica	0.34	0.50
Urease/mica	0.31	0.43
Microtubule/DETA	0.23	0.26

Comparison is of noise on top of the structures with the noise on the supports.

movements, it is important to know the frequencies at which any motion is taking place. In an attempt to answer this question, Fourier analysis was performed on the data.

Fig. 6 shows the fast Fourier transforms of the full data sets shown in Fig. 5. These transforms have been smoothed from the originals by averaging over 10 data point intervals. Generally there is more noise over the proteins than over the supports at frequencies below 200 to 250 Hz. The transforms of the DODAB and its support are very similar (see Fig. 6 *A*), indicating that a soft sample should not affect the noise spectrum per se. These spectra are characterized by white noise above 40 Hz and a sharp rise to the direct current level below this. The narrow peaks visible in many of the spectra, spaced at about 60 Hz, are due to the fundamental line frequency and harmonics of the electricity supply. Comparing the protein spectra, it can be seen that an antibody shows more low-frequency noise, although the support data also exhibit an increase at smaller frequencies (see Fig. 6 *B*). The urease also shows an appreciable amount of movement below 150 Hz (Fig. 6 *C*), and the microtubule only a slight difference (Fig. 6 *D*). A pausible explanation for the interpretation of these data might come from differences in the motion that various types of protein exhibit on the surfaces. However, from these preliminary data it is not possible to ascribe differences in height fluctuations to protein function, because the orientation of the proteins on the surface is unknown.

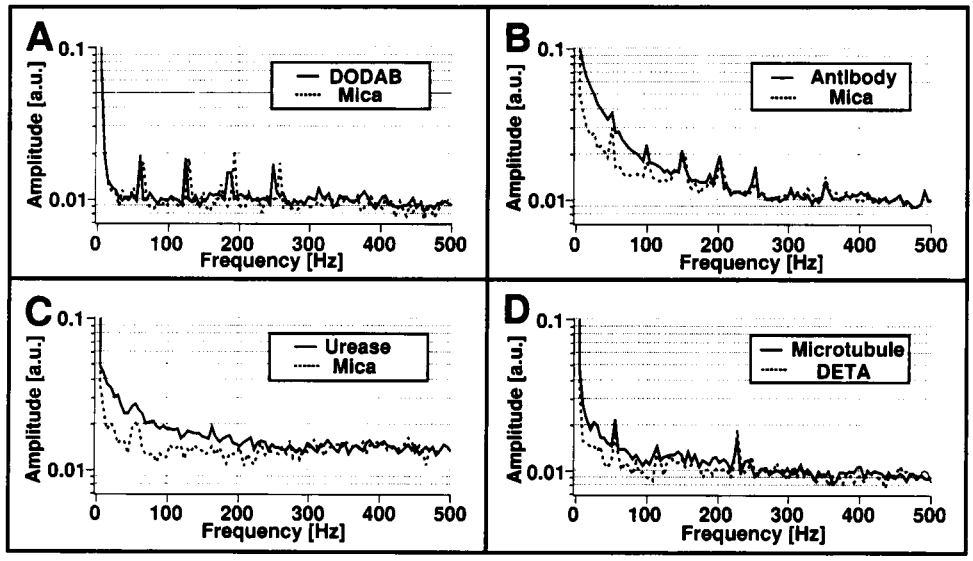

FIGURE 6 Fourier transforms of the full data sets of height fluctuations, 3 s of which are shown in Fig. 5. These are smoothed transforms by averaging over 10-data point intervals. Again it is clear that the most fluctuations occur over the antibody and the fewest over the microtubule. The DODAB spectrum is almost identical to its support. These spectra also suggest that the proteins have fluctuations at characteristic frequencies; the antibody seems to have the greatest fluctuations at low frequencies, below 100 Hz. The urease is different from its support up to about 220 Hz, as is the microtubule, but the difference is less marked. The sharp peaks in the spectra correspond to the characteristic line frequency of the electricity supply and its harmonics. The temporal resolution of these data is about 200 Hz (about 5 ms); above this frequency the protein spectra drop into the background support spectra.

The limit on the temporal resolution of the data sets presented here is about 200 Hz, i.e., 5 ms. Above this frequency the protein noise is comparable to the noise on the support. Data were sampled at a frequency of 1 kHz, which gives a frequency range for the Fourier spectra of 0 to 500 Hz. The sampling frequency was chosen to be well below limits enforced by the tapping frequency. We want to sample the average value of the height response for several taps of the tip on the sample. Cantilevers with higher resonant frequencies will give a better temporal resolution, as they tap faster, enabling sampling at higher rates. However, limitations in temporal resolution will also arise from the response of the feedback loop, the inertia of the piezo tube, and the response time of the cantilever. At higher gain settings a broad peak was sometimes seen at 250 to 300 Hz. This may be a resonance associated with the characteristic response time of the feedback loop. In this case, the piezo will not respond to movements with frequencies greater than this. This puts a limit on observing motions that are shorter than 4 ms.

Control of the gains in these experiments was very important. As mentioned already, if the gain was too high, a resonance peak was observed in the Fourier spectrum. Generally gains did not seem to affect the noise data acquired, provided that the gain was below a certain level. For each sample studied one could increase the gains until a point of instability was reached and then feedback-induced oscillations occurred. All data were taken as close to this point as was practically possible. The gain must be sufficiently high for the tip to be following the motion underneath it correctly. It is conceivable that increases in noise over proteins could be due to differences of the tip following a soft sample. However, this was not observed on the DODAB, and the tip is not scanning while data are collected. Another possibility is that the tip rolls across the curved protein surface, causing apparent low-frequency motion visible in the fast Fourier transforms. The typical drift rates of a few angstroms per second calculated from the *xy*-piezo plots (see Fig. 4 *C*) suggest that this may not be significant.

Another parameter that could affect noise levels was that of the tapping set point, i.e., how hard the tip was tapping the surface. This also in some ways determines how well the tip tracked the sample. At higher set points (lower force), where the tip was only just contacting the sample, the noise would increase dramatically to 1 nm peak to peak, say. All imaging and noise measurements were performed with the tip tapping the surface lightly enough not to remove proteins during scanning but hard enough to enable good tracking of the molecules by the tip. Increasing the force could also cause large increases in noise. All protein data sets were taken directly after collecting data on the support with the same set point and gains. The noise on the support was always used as a way to monitor the applied force and gain settings. The applied force and gains were kept constant between acquisitions of data on the support and on the proteins.

Provided that the above experimental methods were adhered to, the noise data were reproducible. The noise data have been reproduced on independently prepared samples for each of the systems studied. We collected at least four

data sets from at least two different sample preparations. For the antibodies we have seven sets from three preparations and ten sets from ten preparations for the urease. There were times when the data were not reproduced successfully on the protein samples. These data sets were characterized by similar noise on the support and on top of the protein. It was evident from images that these tips were contaminated, probably with protein molecules or fragments picked up from the surface. With protein always between the tip and sample, it is not suprising that the noise characteristics were so similar. The importance of having a clean tip before starting such experiments cannot be overemphasized. Experience showed that cleaning cantilevers in a strong oxidizing agent and then under UV light always gave data with measurable noise differences between the support and protein.

The purpose of this paper is to demonstrate that differences can be observed in height fluctuations above different protein molecules. These height fluctuations may be due to many things: 1) protein conformational change, 2) partial protein rotation on the surface, 3) fluctuations in the protein hydration layer, or 4) tip-induced motion that may depend on the strength of adsorption of the proteins to the supports. There are other possibilities, such as increased noise caused by changes in adhesion as the tip taps over a protein, although previous work has indicated that adhesion over a protein can be lower than the support it is adsorbed to (Radmacher et al., 1994b).

For the longer term goal of relating observed height fluctuations to biological function, it appears necessary to find systems of oriented, active proteins on supports that are flat enough for AFM. Specifically, the roughness of the support must be much less than the size of the protein molecules, so that they can be located on the surface in known orientations.

CONCLUSIONS

The height fluctuations over different proteins have been measured by using an AFM operated in fluid tapping mode. A protein tracking device was set up that can enable the AFM tip to track single protein molecules indefinitely, provided that thermal drift is not too severe. The height fluctuations over individual protein molecules are greater than the height fluctuations over the supports they are adsorbed to. These height fluctuations appear to be due to intrinsic properties of the proteins and not merely to interactions of the tip with a soft sample, as was demonstrated by height fluctuations over the soft amphiphile DODAB that were comparable to those on the mica support. Fourier analysis of the data has shown that different types of proteins exhibit height fluctuations at different frequencies. To determine if the AFM is capable of detecting motions relevant to the biological functions of proteins, it will be necessary to carry out further studies on proteins with known orientations.

We thank Joe Zasadzinski for the use of equipment in his laboratory.

This work is supported by a grant from the Materials Research Division of the National Science Foundation under grant NSF-DMR-9221781. Neil Thomson wishes to thank NATO for his fellowship. Monika Fritz thanks the Deutsche Forschungsgemeinschaft for her fellowship. We thank Digital Instruments for AFM support.

REFERENCES

Bezanilla, M., B. Drake, E. Nudler, M. Kashlev, P. K. Hansma, and H. G. Hansma. 1994. Motion and enzymatic degradation of DNA in the atomic force microscope. *Biophys. J.* 67:2454–2459.

Binnig, G., C. F. Quate, and C. Gerber. 1986. Atomic force microscope. *Phys. Rev. Lett.* 56:930.

Bustamante, C., J. Vesenka, C. L. Tang, W. Rees, M. Guthold, and R. Keller. 1992. Circular DNA molecules imaged in air by scanning force microscopy. *Biochemistry.* 31:22–26.

Butt, H.-J., P. Siedle, K. Seifert, K. Fendler, T. Seeger, E. Bamberg, A. L. Weisenhorn, K. Goldie, and A. Engel. 1993. Scan speed limit in atomic force microscopy. *J. Microsc.* 169:75–84.

Cleveland, J. P., S. Manne, D. Bocek, and P. K. Hansma. 1993. A nondestructive method for determining the spring constant of cantilevers for scanning force microscopy. *Rev. Sci. Instrum.* 64:403–405.

Dreier, M., D. Anselmetti, T. Richmond, U. Dammer, and H.-J. Guntherodt. 1994. Dynamic force microscopy in liquids. *J. Appl. Phys.* 76:5095–5098.

Dye, R. B., S. P. Fink, and R. C. Williams. 1993. Taxol-induced flexibility of microtubules and its reversal by MAP-2 and Tau. *J. Biol. Chem.* 268:6847–6850.

Florin, E.-L., V. T. Moy, and H. E. Gaub. 1994. Adhesion forces between individual ligand-receptor pairs. *Science.* 264:415–417.

Frauenfelder, H., S. G. Sligar, and P. G. Wolynes. 1991. The energy landscapes and motions of proteins. *Science.* 254:1598–1603.

Frauenfelder, H., and P. G. Wolynes. 1994. Biomolecules: where the physics of complexity and simplicity meet. *Phys. Today.* 47:58–64.

Fritz, M., M. Radmacher, J. P. Clevelend, M. W. Allersma, R. J. Stewart, R. Gieselmann, P. Janmey, C. F. Schmidt, and P. K. Hansma. 1995. Imaging globular and filamentous proteins in physiological buffer solutions with tapping mode atomic force microscopy. *Langmuir.* 11: 3529–3535.

Han W. H., J. X. Mou, J. Sheng, J. Yang, and Z. Shao 1995. Cryo atomic force microscopy—a new approach for biological imaging at high resolution. *Biochemistry.* 34:8215–8220.

Hansma, H. G., and J. H. Hoh. 1994. Biomolecular imaging with the atomic force microscope. *Annu. Rev. Biophys. Biophys. Chem.* 23: 115–139.

Hansma, P. K., J. P. Cleveland, M. Radmacher, D. A. Walters, P. Hillner, M. Bezanilla, M. Fritz, D. Vie, H. G. Hansma, C. B. Prater, J. Massie, L. Fukunaga, J. Gurley, and V. Elings. 1994. Tapping mode atomic force microscopy in liquids. *Appl. Phys. Lett.* 64:1738–1740.

Jabri, E., M. B. Carr, R. P. Hausinger, and P. A. Karplus. 1995. The crystal structure of urease from Klebsiella aerogenes. *Science.* 268:998–1004.

Johnson, L. N. 1992. Time-resolved protein crystallography. *Protein Sci.* 1:1237–1243.

Karrasch, S., R. Hegerl, J. H. Hoh, W. Baumeister, and A. Engel. 1994. Atomic force microscopy produces faithful high-resolution images of protein surfaces in an aqueous environment. *Proc. Natl. Acad. Sci.* 91:836–838.

Lee, G. U., L. A. Chrisey, and R. J. Colton. 1994. Direct measurement of the forces between complementary strands of DNA. *Science.* 266: 771–773.

Okuyama, K., Y. Soboi, N. Iijima, K. Hirabayashi, T. Kunitake, and T. Kajiyama. 1988. Molecular and crystal structure of the lipid-model amphiphile Dioctadecyldimethylammonium bromide monohydrate. *Bull. Chem. Soc. Jpn.* 61:1485–1490.

Parak, F., and H. Frauenfelder. 1993. Protein dynamics. *Phys. A.* 201: 332–345.

Petsko, G. A., and D. Ringe. 1984. Fluctuations in protein structure from x-ray diffraction. *Annu. Rev. Biophys. Bioeng.* 13:331–371.

Putman, C. A. J., K. O. Vanderwerf, B. G. DeGrooth, N. F. Vanhulst, and J. Greve. 1994. Tapping-mode atomic force microscopy in liquid. *Appl. Phys. Lett.* 64:2454–2456.

Radmacher, M., M. Fritz, J. P. Cleveland, D. R. Walters, and P. K. Hansma. 1994a. Imaging adhesion forces and elasticity of lysozyme adsorbed on mica by atomic force microscopy. *Langmuir.* 10: 3809–3814.

Radmacher, M., M. Fritz, H. G. Hansma, and P. K. Hansma. 1994b. Observation of enzyme activity with the atomic force micrscope. *Science.* 265:1577–1579.

Reithel, F. J. 1971. Ureases. *In* The Enzymes. Academic Press, New York and London. 1–21.

Rugar, D., and P. K. Hansma. 1990. Atomic force microscopy. *Phys. Today.* 43:23–30.

Schabert, F. A., C. Henn, and A. Engel. 1995. Native *Escherichia coli* OmpF porin surfaces probed by atomic force microscopy. *Science.* 268:92–94.

Steinbach, P. J., A. Ansari, J. Berendzen, D. Braunstein, K. Chu, B. R. Cowen, D. Ehrenstein, H. Frauenfelder, B. J. Johnson, D. C. Lamb, S. Luck, J. R. Mourant, G. U. Neinhaus, P. Ormos, R. Philipp, A. Xie, and R. D. Young. 1991. Ligand binding to heme proteins: connection between dynamics and function. *Biochemistry.* 30:3988–4001.

Venier, P., A. C. Maggs, M.-F. Carlier, and D. Pantaloni. 1994. Analysis of microtubule rigidity using hydrodynamic flow and thermal fluctuations. *J. Biol. Chem.* 269:13353–13360.

Williams, R. C. J., and J. C. Lee. 1982. Preparation of tubulin from brain. *Methods Enzymol.* 85:376–385.

Yang, J., J. Mou, and Z. Shao. 1994. Molecular resolution atomic force microscopy of soluble proteins in solution. *Biochim. Biophys. Acta.* 1199:105–114.

Young, R. D., H. Frauenfelder, B. J. Johnson, D. C. Lamb, G. U. Nienhaus, R. Philipp, and R. Scholl. 1991. Time and temperature dependence of large-scale conformational transitions in myoglobin. *Chem. Phys.* 158: 319–327.